

# Digital Image Correlation Strain Measurement of Thick Adherend Shear Test Specimen Joined with an Epoxy Film Adhesive

J.Kosmann\*, O.Völkerink, M.J. Schollerer, D. Holzhüter, C. Hühne

*German Aerospace Center, Institute for Composite Structures and Adaptive Systems,*

*Lilienthalplatz 7, D-38108 Braunschweig, Germany*

---

## Abstract

Structural bonding and bonded repairs of composite materials become more and more important. Understanding the strain within the bondline leads to suitable bonding design. For new design approaches the strain distribution within the bondline has to be analyzed. Thus, often finite element analysis (FE) are used. However, a huge challenge is the availability of reliable material properties for the adhesives and their validation. Previous work has shown that it is possible to measure the small displacements resulting within thin epoxy film adhesives using high resolution digital image correlation (DIC). In this work a 2D DIC setup with a high resolution consumer camera is used to visualize the strain distribution within the bondline over the length of the joint as well as over the adhesive thickness. Therefore, single lap joints with thick aluminum adherends according to ASTM D 5656 are manufactured and tested. Local 2D DIC strain measurements are performed and analyzed. Two different camera setups are used and compared. The evaluation provides reliable material data and enables a look insight the bondline. The results of the full field strain data measured with DIC are compared with numerical simulations. Thus, material models as well as chosen parameters for the adhesive are validated. Compared to extensometers, giving only point-wise information for fixed measuring points, the DIC allows a virtual point-wise inspection along the complete bondline. Furthermore, it allows measuring close to the bondline to reduce the influence of adherend deformation.

---

\* Corresponding author. Tel.: +49 -531-295-2087; fax: +49-531-295-3035.  
E-mail address: jens.kosmann@dlr.de.

25 **1. Introduction**

Structural bonding and bonded repairs of composite materials become more and more important. However bonded joints in present structural applications do not utilize their full load carrying potential. A huge challenge is the availability of reliable material properties for the adhesives, see [1]–[3]. Budhe et al. [4] investigated performance parameters and environmental factors affecting the strength of a joint. However to analyze the strain distribution within the bondline often finite element (FE) analysis are used. Ongoing research improves the FE analysis but the reliable prediction of stress and strength of a joint is still challenging [5]. For this reason a validation of the FE results is needed. Understanding the strain within the bondline leads to suitable bonding design. Kunz et al. [6] performed local displacement measurements insight the bondline using particle tracking and in situ computed tomography, however this is only applicable for thicker bondlines. Kosmann et al. [7] has shown that it is possible to measure the small displacements resulting with thin epoxy film adhesives using high resolution digital image correlation. The next step is to visualize the strain distribution within the bondline over the length of the joint as well as over the adhesive thickness. Therefore, the measuring resolution is critical for reliable results. Previous work has shown that this is possible with 2D DIC [8]. The full field measuring possibilities help to improve the joint design and developing stress peak reducing concepts by using a toughening of the joint surface [9]. Compared to extensometers, giving only point-wise information for fixed measuring points, the DIC allows a virtual point-wise measuring along the complete bondline. It allows a measuring close to the bondline to reduce the influence of adherend deformation. As commercial digital Image correlation systems are limited in camera resolution the investigation here is to use standard consumer camera system for image recording.

45 In this work single lap joints with thick aluminum adherends according to ASTM D 5656 [10] are tested. Local 2D DIC strain measurements are performed and analyzed. The results of the full field stain data measured with digital image correlation are compared with numerical simulations. Thus, material models and chosen parameters for the adhesive can be validated. . Compared to extensometers, giving only point-wise information for fixed measuring points, the DIC allows a virtual point-wise inspection along the complete bondline. Furthermore, it allows a measuring close to the bondline to reduce the influence of adherend deformation.

50

## 2. Experimental Work

### 2.1. Specimen Manufacture

55 Within this section the measurement of thick adherend shear test specimen (TAST) is described. The TAST  
specimen are manufactured according to ASTM D 5454-04 [10]) and joined with an epoxy film adhesive. The  
used adhesive is the LOCTITE EA 9695 050 NW AERO epoxy film adhesive[11]. The adherends are made  
out of aluminum sheets (EN AW 5083). The geometry of the TAST is shown in Figure 1. Prior bonding the  
60 surface is sandblasted using white corundum grade F180 followed by cleaning with acetone and isopropyl  
alcohol. Following to the surface preparation, the adhesive film is applied and the stack is consolidated for  
one hour using a vacuum bag. The subsequent curing is performed in a heat press. The used heat press is  
equipped with a vacuum tight press chamber. The temperature of 130°C and pressure of 0.1MPa is according  
to the data sheet of the adhesive. Afterwards, the plates are cut in strips, providing a set of seven specimen  
blanks. Each specimen is then CNC milled to the exact contour including the holes for clamping, shown in  
65 Figure 1. For the work presented two sets with seven specimens each are produced. The cured adhesive  
thickness of one ply film adhesive is between 100 to 150  $\mu\text{m}$ . However for reliable bondline thickness data  
each specimen is determined and documented using a calibrated microscope. The first series is made with one  
ply adhesive resulting in an average thickness of  $t_b = 0.117$  mm, the second series is bonded with two plies  
of adhesive, resulting in  $t_b = 0.21$  mm.

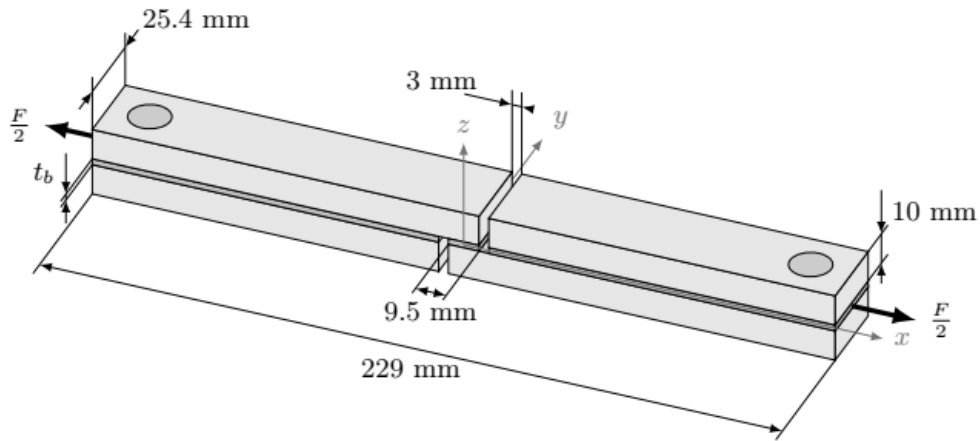


Figure 1: TAST Specimen Geometry

75 *2.2. Experimental test setup*

The tensile testing of the TAST specimen is performed at controlled room temperature conditions using universal testing machines by Zwick (Zwick 1476 and Zwick 1484). The crosshead speed was 0.05 in/min and kept constant throughout all tests. The testing machines have a digital control unit and are equipped with a 100kN respectively 250kN Load cell.

80 *2.3. Digital Image Correlation Strain Measurement*

In addition to the load- displacement data of the testing machine, digital image correlation (DIC) technology is used to measure the TAST specimen. Kosmann et al [8] have shown that high resolution DIC is feasible using the standard 12MPixel ARAMIS system by GOM. However, for an even closer look a higher resolution is mandatory. For the presented work the data for the DIC are recorded with a consumer full-frame mirrorless camera with a resolution of 42 mega pixel. The model used is a Sony  $\alpha$ 7RIII camera. The fixture of the camera setup, shown in Figure 2, is mounted on the moving traverse of the testing machine. This provides as small relative movement of camera and specimen as possible. The camera is mounted on a macro slide to enable a precise focusing of the specimen.

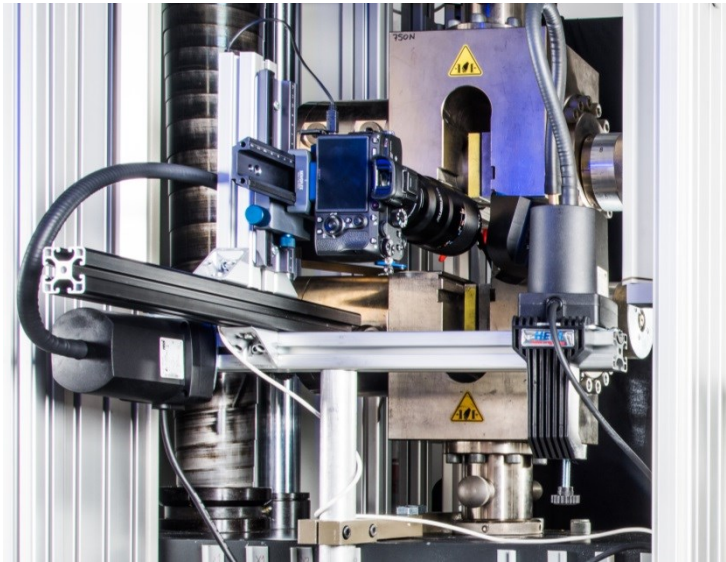


Figure 2: Measurement setup of DIC system

For the measurements two different lens setups are used. In the first setup the FE 90 mm macro Lens from Sony is used. In the second setup a magnifying lens from Canon type MP-E 65mm is used. With these two different lenses two measuring areas are realized as shown in Figure 3. The first setup is used to gain general material data and provides an overview over the complete adhesive area. The measuring area is 18 mm by 11mm. With the second setup the the measuring area is 7.2mm by 4.8mm hence the resolution of the bondline is even better. These results are compared with strain distributions from detailed FE simulations by Völkerink et al. [12].

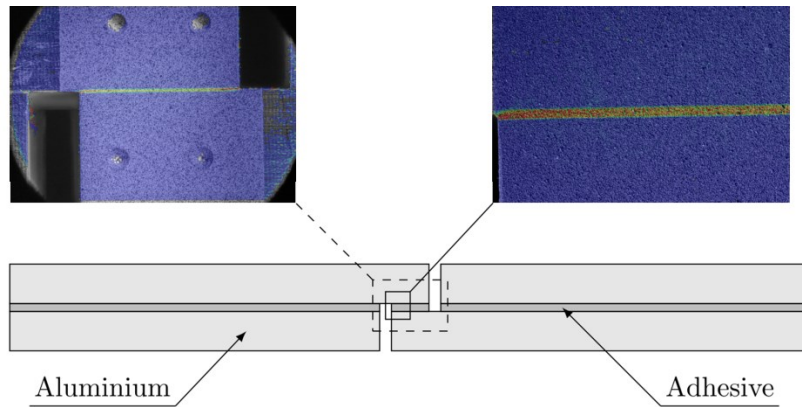


Figure 3: Two measuring areas on the TAST specimen

To record the images the camera is controlled with a self-developed control unit. With the control unit the camera is triggered at selected frequencies. Additionally the unit records the analog force and displacement data output from the testing machine. This allows a correlation of the images taken by the camera with the force data recorded by the testing machine. One additional feature is a 2<sup>nd</sup> measuring frequency triggered either manual or automatically when reaching a predefined force value. With this 2<sup>nd</sup> frequency a higher frame rate closed to the specimen failure can be recorded without running into buffer memory overflow of the camera. The starting frequency used in this test campaign is 2 Hz using single shot mode. Reaching the defined load of 10kN the software changes the mode to the fast continuous shooting mode. In this mode the picture rate is around 8 Hz. With automatically generated python scripts the recorded images are imported into the DIC software. Within this work the GOM Correlate Professional 2018 is used for the DIC evaluation.

### 3. Results

#### 3.1. Material data evaluation

For material characterization the first camera setup capturing the full overlap area is used. All seven specimens of the first series, bonded with one layer of adhesive film, are tested in this configuration.

After test and creation of the GOM Correlate files two manual steps for data evaluations are necessary. The

first step is to set the coordinate system. The origin of the system is in one corner and in the middle of the bondline, the x axis parallel to the bondline, the y axis in plane of the viewing surface and the z axis is out of plane. Second step is the calibration of the scale with one point on each side of the lab. The calibration is necessary as this 2D setup is not calibrated as a 3D DIC measurement would be. With a stereoptical 3D DIC setup a calibration of the camera setup with known calibration objects is possible. Measuring only 2D the missing third dimension does not allow this kind of calibration as the out of plane direction is not captured. After these manual steps all subsequent steps are automated. The first step is to fit the measured data onto a 3D model of the specimen. The 3D model defines the point positions for the evaluation. Second step is to create five virtual cuts parallel to Y axis.

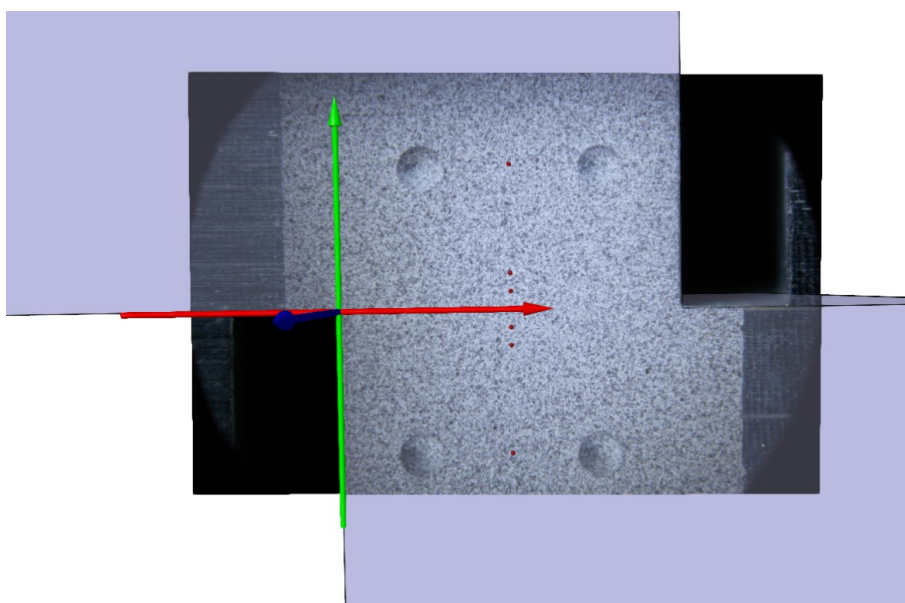


Figure 4: DIC Measurement with coordinate system and CAD model

The evaluation of the adhesive data is based on a calculation of single measurement points as Kosmann et al. [7] already used for the evaluation of adhesive properties with tubular butt joints. The points, shown in Figure 5, are defined as: Point 4 is at the middle of the bondline, point 3 and 5 are close to the bondline with a distance of 0.5 mm. Point 2 and 6 are another 0.5 mm away. Point 1 and 7 are 3.0mm away from the adhesive and represent the distance a clamping extensometer would have. The five cuts are equally distributed over the

lab starting 0.15 mm from the tip; cut\_x\_4.750 mm is a cut through the middle of the 9.5 mm overlap. Figure 6

135 shows the distance measuring between the selected points.

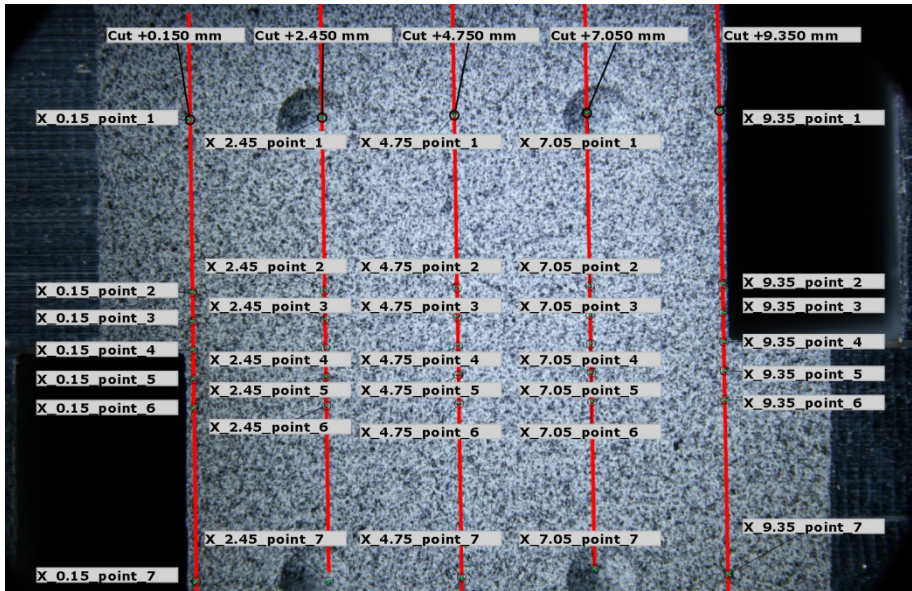


Figure 5: Points and cuts used for evaluation

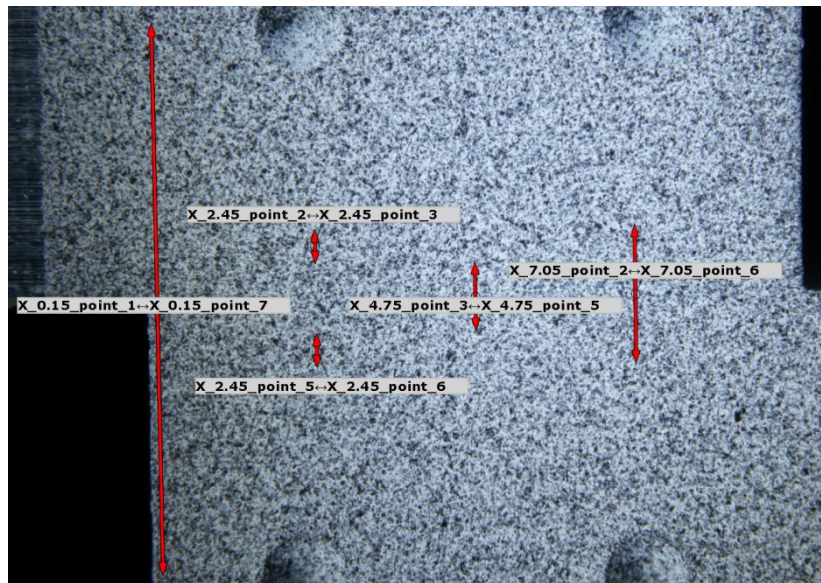


Figure 6: Distance measuring between points

140 The displacement information of each point in each direction together with the distance between the points is



exported for every image. The subsequent evaluation is processed using a python script. For calculation of the  $\tau$ - $\gamma$  values the measured shear deformation has to be corrected by the deformation of the adherend. Herein this work the adherend deformation is calculated for each adherend in each load step separately. This approach provides several advantages: No additional reference specimen is necessary. Adherend deformation is measured next to the loaded interface. Capturing the influence of different adherend materials. Non sensitive of asymmetry. The adhered deformation  $\gamma_{adh1}$  and  $\gamma_{adh2}$  is calculated using the relative movement between point 2 and 3, respectively point 5 and 6, within each adherend normalised with the point distance  $Dist_{P2P3}$  and  $Dist_{P5P6}$ . The  $\gamma_{adhesive}$  value is calculated using point 3 and 5 next to bondline and referenced to the adhesive thickness  $T_{adhesive}$ .

$$\gamma_{adh1} = \frac{P2x - P3x}{Dist_{P2P3}}$$

$$\gamma_{adh2} = \frac{P5x - P6x}{Dist_{P5P6}}$$

$$\gamma_{adhesive} = \frac{(P3x - P5x) - \gamma_{adh1} * 0,5 * (Dist_{P3P5} - T_{adhesive}) - \gamma_{adh2} * 0,5 * (Dist_{P3P5} - T_{adhesive})}{T_{adhesive}}$$

As DIC data include some noise different filter options are available in the GOM Correlate Software. The filters are applied on the evaluation of the single point inspections. Each filter is based on the information of one time step before and after the actual value. In Figure 7 the effect of the filter is shown and summarized in Table 1. It can be seen, that each filter cuts off the last measuring points. The median filter has nearly no effect on the noise but has a big cut off. The average and spline filter both give smooth results with a good fit of the raw data. The average filter has a bigger cut off then the spline filter. The Thus, the spline filter is used for the ongoing evaluation.

Table 1: Overview of different filter types

Filter	Pro	Contra
No Filter	exact measuring data	high noise

Median Filter	[-]	big cut off high noise
Average Filter	good smoothing good fit	medium cutoff
Spline Filter	good smoothing good fit lowest cut off at the end	still some cut of

160

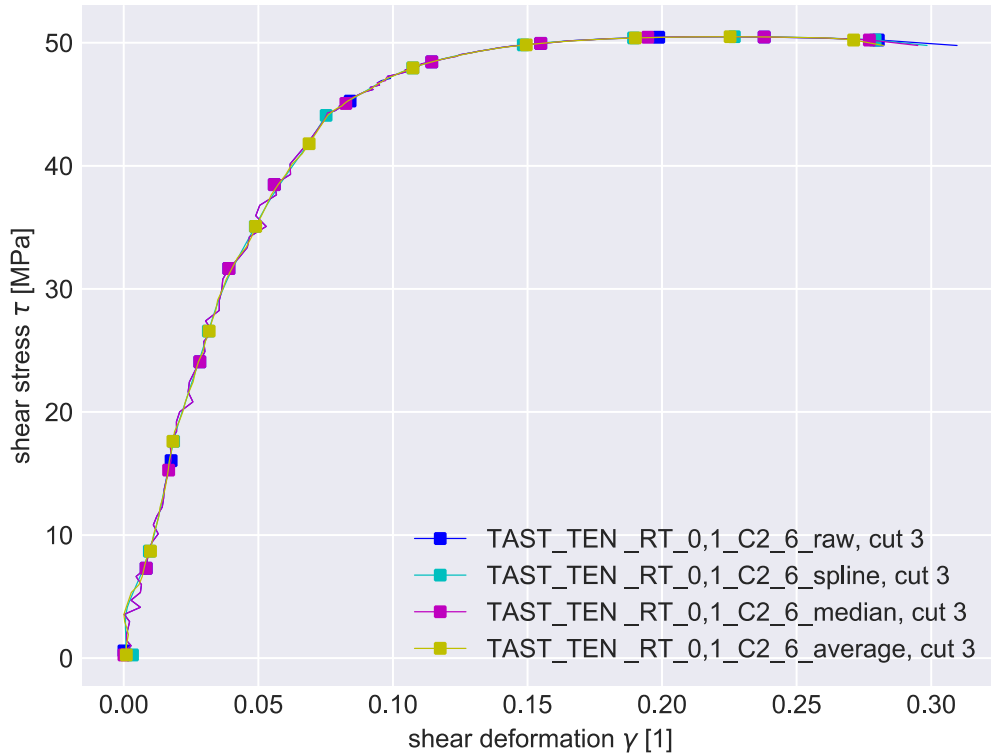


Figure 7: Comparison of different filter within GOM Correlate

With the described cuts perpendicular to the bondline and evenly distributed over the length, see Figure 5, the effect of different measuring positions over the length of the bondline can be analysed. Figure 8 shows the results of specimen 7. It is clearly shown that each cut has a different result for the shear stress -shear strain result as known from literature [13], [14]. Cut 3 in the middle of the overlap, compared to both outer cuts 1 and 5 has a higher stiffness and less deformation, the reason for this can be seen in the detailed bondline inspection in section 3.2. The symmetric cuts 1 and 5 respectively 2 and 4 showing a good symmetry of the measured data. For further inspections only the middle cut 3 is used

165

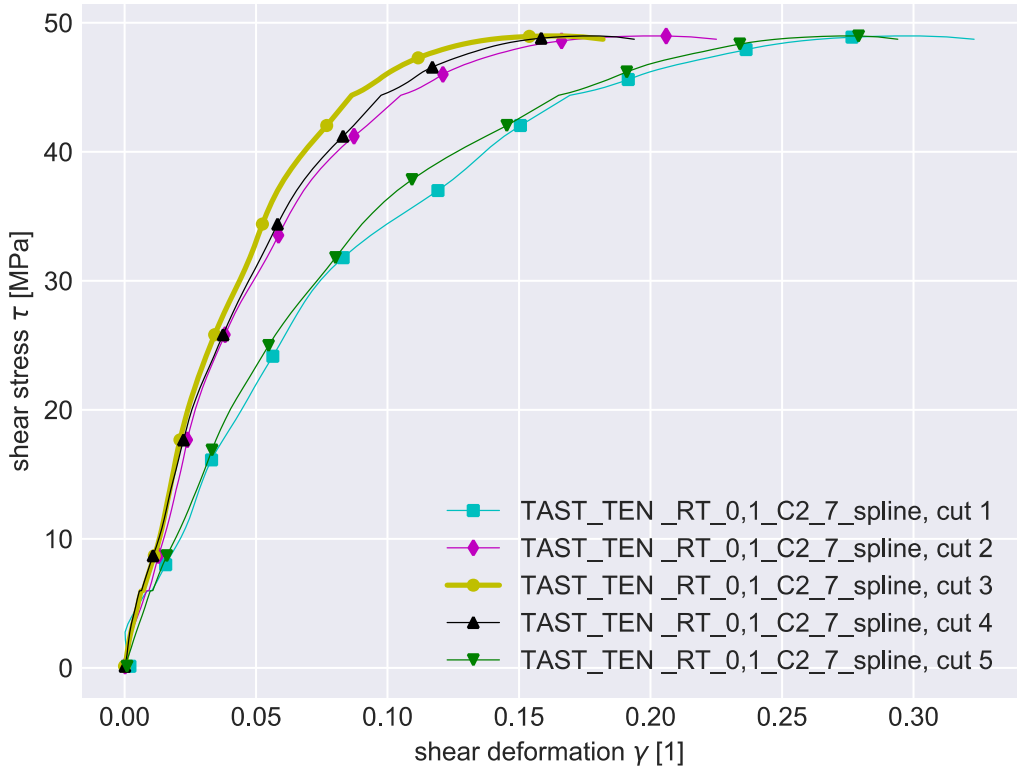


Figure 8: Comparison of different cuts over the bondline

All seven tested specimens within this series are evaluated at the middle cut using the presented filter settings.

The results are plotted in Figure 9. All Specimen show a linear elastic at first and second a plastic material behaviour as it is expected for this adhesive type [7]. Yielding starts between 30 MPa and 40MPa. The shear

failure strength is between 48 MPa and 52 MPa. However the results for the failure shear deformation show a wide variation between 0.18 and 0.32. The obtained data can be used to calculate a hardening curve as Input for detailed FE modelling.

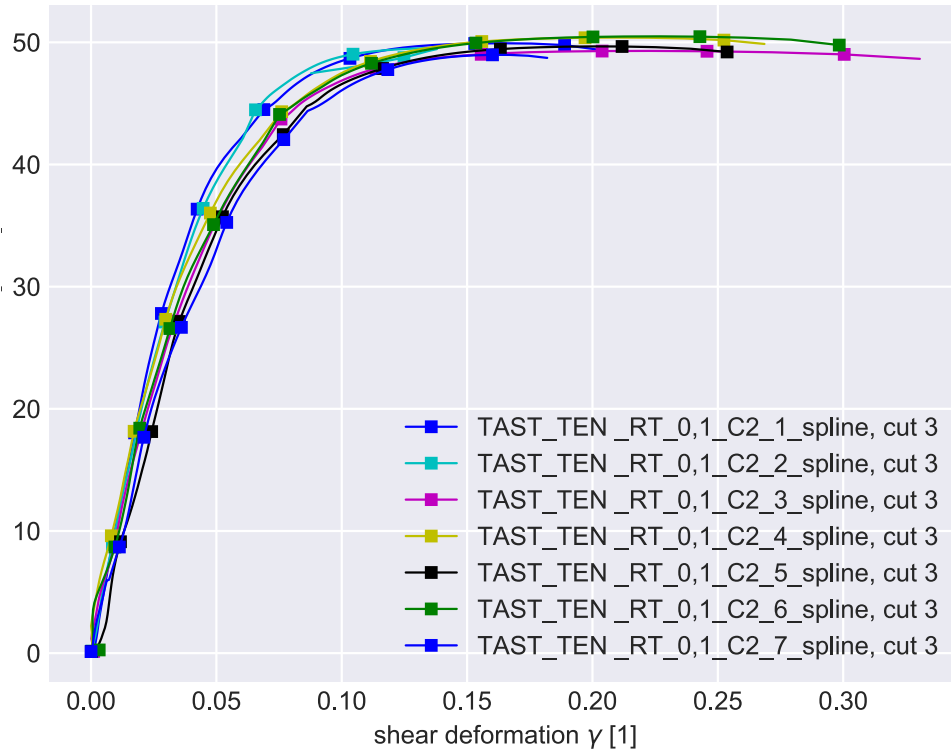


Figure 9: Shear stress - shear strain diagram of all 7 specimen spline filtered for Cut 3

180 Another possible inspection due to the high resolution of the camera is the full field analysis. Figure 10 presents the calculated von Mises strain in the bondline of the TAST specimen. The strain peaks on both corners as well as the strain distribution over the bondline length can be seen. This is similar to the inspection of the different cuts in Figure 8. However, as this is assumed to be symmetric over the bondline, a detailed measurement of one half of the specimen is sufficed. This is realized with the second camera setup, enabling  
 185 an even closer look, the results are described below.

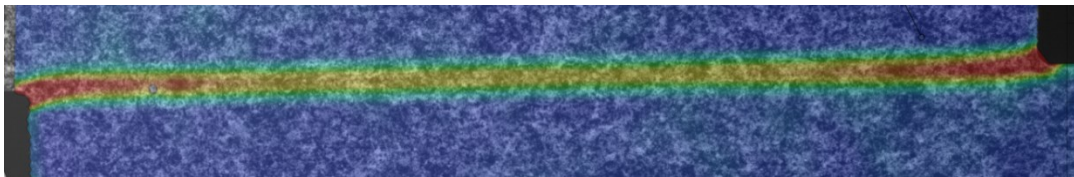


Figure 10: von Mises strain in TAST specimen bondline

### 3.2. Detailed bondline inspection and comparison to FEM

For a more detailed bondline inspection and a direct comparison to the FE results by Völkerink et al. [12] the second camera setup with a higher magnification is used. The focus for this setup is not a pointwise inspection as described above but a full field inspection within the bondline. The high resolution of the camera combined with the magnifying lens allows a detailed measuring within the bondline. The tested specimens with this setup are bonded with two plies of the epoxy film adhesive. Hence the thickness of bondline is about 0.2mm.

For the visual inspection of the DIC results here the  $\epsilon_{xy}$  strain results are plotted for three load steps. With an increasing load level the strain values are also increasing. However, it can be seen clearly, that there is a strain peak next to the tip of the overlap.

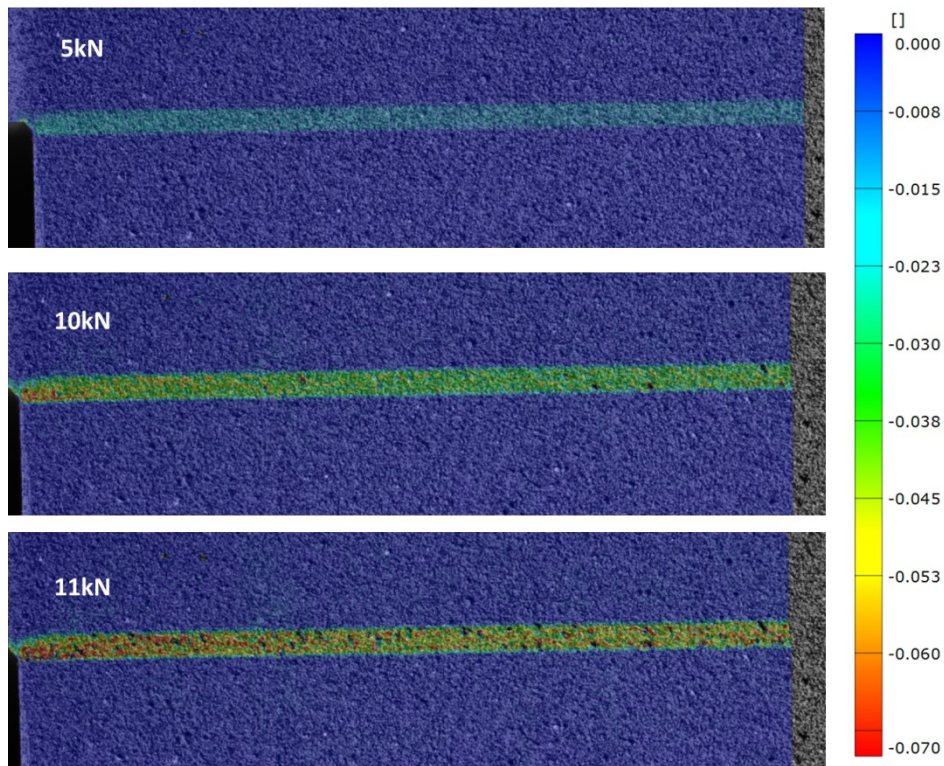


Figure 11: Detailed bondline measurement; plot of  $\epsilon_{xy}$  strain for 5kN, 10kN and 11kN

For a more detailed inspection the strain values on cuts are analyzed. Within the bondline one cut in the Y-

plane and three cuts in the X-plane orthogonal to the bondline, visualized in Figure 12, are exported. The cut  
in Pos.1 is next to the overlap tip, Pos.2 1.5mm from the tip and cut three in the middle of the overlap.

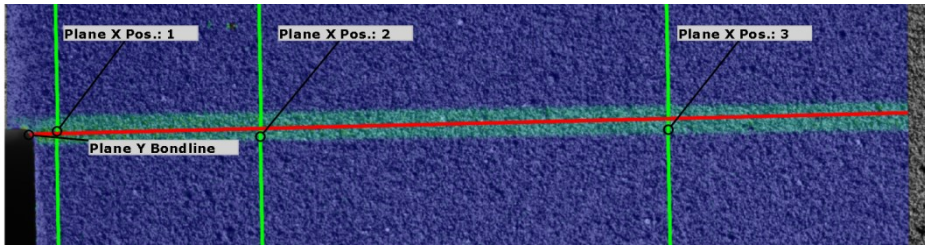


Figure 12: Detailed bondline measurement, cut trough bondline in X and Y plane

The strain values for the cuts in the X-plane provide the strain distribution over the adhesive thickness and in  
the adherends. Viewing the cut next to the edge an asymmetrical distribution of the strain can be observed. A  
high strain peak on the adherend tip compared to a lower strain level on the side of the loaded adherend  
occurs. It indicates the stress concentration of the notch effect. Locking further away from the notch towards  
the middle of the overlap the strain distribution becomes symmetrical. The lowest values can be found in the  
middle of the overlap.

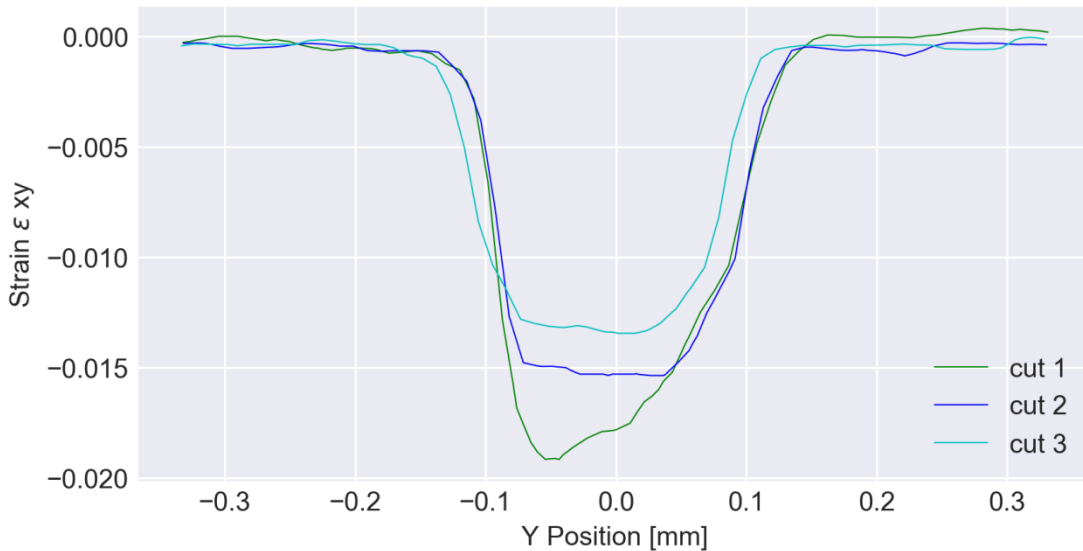


Figure 13:  $\epsilon_{xy}$  Strain over adhesive thickness at 6kN

The Y-plane cut provides the strain distribution in the middle of the bondline along the overlap. Völkerink et al. [12] modeled and calculated the TAST specimens tested in this work. As an excerpt a comparison of the DIC and FEM is presented in Figure 14. However using DIC measuring it is only possible to measure on the side surface of the specimen. This has to be considered when comparing to FE or analytical calculations. Within this work only the von Mises results on the outer surface of a 3D FE model are shown. The FE analysis is calculated with the material data given in Table 2.

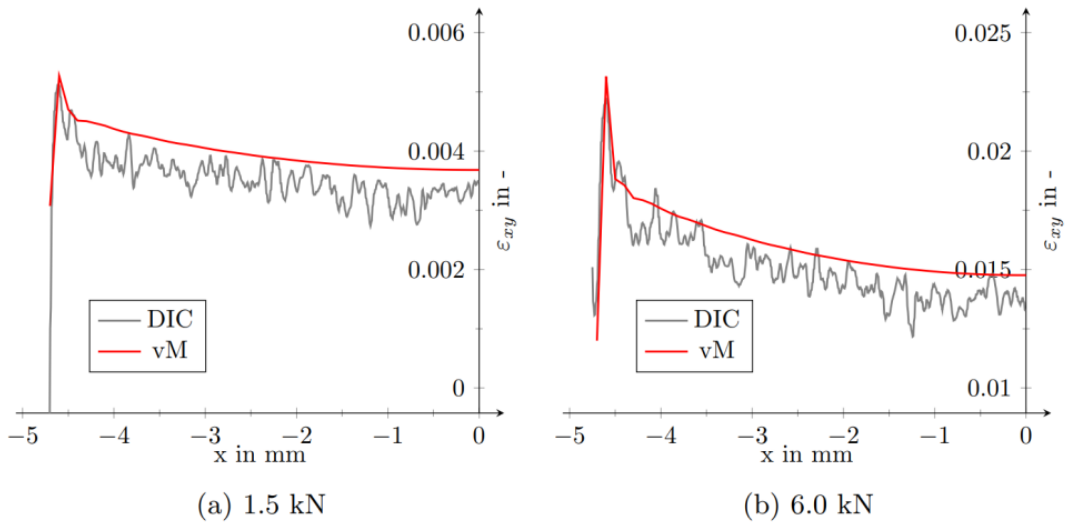


Figure 14: DIC - FE  $\epsilon_{xy}$  Strain comparison at 1.5kN (a) and 6kN (b)

In Figure 14 the results for the  $\epsilon_{xy}$  distribution along the bondline for two loads is shown. The strain is plotted from the edge of the bondline at  $x = -4.75$  mm until the half overlap length  $x = 0$  mm. Both DIC and FE values are calculated in the facet respectively element along the middle of the bondline. In both load steps it can be seen that there is some noise in the DIC data. The FE result slightly overestimates the strain but is in good agreement.

Table 2: Properties of Loctite EA 9695 050 NW AERO epoxy film adhesive; Material data from Literature [15]–[17]), [7]

Property	
Young's modulus, $E$ [MPa]	2205
Poisson's ratio, $\nu$ [-]	0.36
Tensile yield strength, $\sigma_y$ [MPa]	46
Tensile failure strength, $\sigma_f$ [MPa]	51

Shear yield strength, $\tau_y$ [MPa]	33
Shear failure strength, $\tau_f$ [MPa]	52
Fracture toughness in tension, $G_{IC}$ [N/mm]	1.02
Fracture toughness in shear, $G_{IIIC}$ [N/mm]	0.78

#### 4. Conclusion

The results show that the DIC measurement has the capability to provide high resolution strain data. Two different lens setups are shown. The first enables to measure displacement data within a measuring area over the complete bondline length. The second offers to strain measuring directly within the adhesive in the through-thickness direction of the bondline. The used pointwise inspection has the advantage of direct adherend compensation. Furthermore the effect of the nonlinear strain distribution both over the bondline length as well as over the bondline thickness can be measured.

The following conclusions can be drawn:

1. The bigger measurement area provides reliable data to calculate material data with an load dependent correction of the adherend deformation
2. The detailed measuring area allows measuring the strain directly within the bondline without adherend deformation.
3. The strain directly obtained within the middle of the bondline can be used to validate detailed FE analyses.

Based on the conducted experiments it is planned to compare the strain data with a new developed extensometer based on contactless capacitive sensors.

##### 4.1.1. References

- [1] J. Wölper, T. Löbel, J. Kosmann. 3rd international conference on structural adhesive bonding AB 2015, Porto 2015; p 50.
- [2] Wang, C. H.; Chalkley, P. Plastic yielding of a film adhesive under multiaxial stresses. *Int. J. Adhes. Adhes.* **2000**, *20* [2], 155–164. DOI: 10.1016/S0143-7496(99)00033-0.



- [3] da Silva, L. F. M. *Failure strength tests, in Handbook of Adhesion Technology*. da Silva, L. F. M.; Öchsner, A.; Adams, R. D.; Springer: Heidelberg, 2018.
- 255 [4] Budhe, S.; Banea, M. D.; de Barros, S.; da Silva, L. F. M. An updated review of adhesively bonded joints in composite materials. *Int. J. Adhes. Adhes.* **2017**, *72*, 30–42. DOI: 10.1016/j.ijadhadh.2016.10.010.
- [5] da Silva, L. F. M.; Campilho, R. D. S. G. *Advances in numerical Modelling of Adhesive Joints*; Springer: Heidelberg, 2011.
- [6] Kunz, H.; Stammen, E.; Dilger, K. Local displacement measurements within adhesives using particle tracking and In Situ computed tomography. *J. Adhes.* **2015**, *93* [7], 531–549. DOI: 260 10.1080/00218464.2015.1113526.
- [7] Kosmann, J.; Klapp, O.; Holzhüter, D.; Schollerer, M. J.; Fiedler, A.; Nagel, C.; Hühne, C. Measurement of epoxy film adhesive properties in torsion and tension using tubular butt joints. *Int. J. Adhes. Adhes.* **2018**, *83*, 50–58. DOI: 10.1016/j.ijadhadh.2018.02.020.
- 265 [8] J. Kosmann, T. Löbel, D. Holzhüter, C. Hühne and M. Schollerer<sup>1</sup>. High resolution digital image correlation strain measurements of adhesively bonded joints. *ECCM17 - 17th European Conference on Composite Materials*, 2016.
- [9] Schollerer, M. J.; Kosmann, J.; Völkerink, O.; Holzhüter, D.; Hühne, C. Surface Toughening – A Concept to Decrease Stress Peaks in Bonded Joints. 2018 submitted to *J. Adhes.* DOI: 270 10.1080/00218464.2018.1555041.
- [10] D14 Committee. *Test Method for Thick-Adherend Metal Lap-Shear Joints for Determination of the Stress-Strain Behavior of Adhesives in Shear by Tension Loading*, 04th ed.; ASTM International: West Conshohocken, PA, 2017. [D 5656].
- [11] Henkel. Hysol EA 9695 Datasheet. 2018.
- 275 [12] Völkerink, O.; Kosmann, J.; Schollerer, M. J.; Holzhüter, D.; Hühne, C. Strength Prediction of

Adhesively Bonded Single Lap Joints with the eXtended Finite Element Method. 2018 submitted to *J. Adhes.* DOI: 10.1080/00218464.2018.1553120.

[13] M. Goland and E. Reissner. The stresses in cemented joints. *J. Appl. Mech.* 1944, No. 66, A17-A27.

[14] O. Volkersen. Die Nietkraftverteilung in zugbeanspruchten Nietverbindungen mit konstanten Laschenquerschnitten. *Luftfahrtforschung*. 1938, No. 15, 41–47.

[15] Floros, I.; Tserpes, K.; Löbel, T. Mode-I, mode-II and mixed-mode I+II fracture behaviour of composite bonded joints: Experimental characterization and numerical simulation. *Composites, Part B* 2015, *Engineering* 78, 459–468.

[16] Nagel, C.; Klapp, O. Yield and fracture of bonded joints using hot-curing epoxy film adhesive - multiaxial test and theoretical analysis. *International Symposium on Sustainable Aviation 2018*.

[17] Holzhüter, D.; Wilken, A. *Einfluss von Umgebungsbedingungen auf die Festigkeit geklebter lagenvariabler Schäftverbindungen* IB 131-2015 / 15: Braunschweig, 2015.